IJPAC
© Global Research Publications

Vol. 9 • No. 3 • July-September 2014
pp. 127-137

Phase Behaviour, Molecular Interaction and Morphological Studies on Co-crystals of Nicotinamide-p-Nitroaniline Drug System

Vishnu Kant* **and H. Shekhar**

Department of Chemistry, V. K. S. University, Ara-802301, India

ABSTRACT: Present study reports the thermodynamic and interfacial investigation of pharmaceutical active Nicotinamide (NA) – p-Nitroaniline (pNA) binary drug system. The liquidus and solidus equilibrium temperatures of solid dispersions of the system determined by Thaw melt method construct the corresponding solid-liquid phase diagram which exhibit eutectic behaviour at 0.420 mole fraction of p-nitroaniline and 102°C of melting temperature with 1:4 an additive co-crystal having incongruent melting at 131°C and a peritectic 0.674 mole fraction of p-nitroaniline at 130°C. Thermodynamic properties such as excess and mixing functions have been studied for better understanding about molecular interaction, ordering and stability in the system. The value of radius of critical nucleus (r*) of solid dispersions has been found in *nm* scale which suggests new dimensions of solidification process for production of *nano* solid drug dispersions and surprisingly it could be for the better future for global pharmaceutical market. The solid-liquid interface energy (σ), grain boundary energy (σ_{gb}), the Gibbs-Thomson coefficient (τ), the driving force of nucleation (ΔG_v) and the critical free energy of nucleation (ΔG^*) of all drug solid dispersions have been highlighted. Interface morphology of drug solid dispersions follows the Jackson's surface roughness (α) theory and the observed microstructures of parent component and eutectic favours the appearance of anisotropic faceted growth ($\alpha > 2$).

Keywords: Phase diagram, Binary drug, Thermodynamic excess and mixing functions, Critical radius, Microstructure

INTRODUCTION

Currently, interest in binary drug for new pharmaceutical development[1-4] has been increasing due to low solubility, bioavibility and dissolution rate of poorly soluble of the pure drug candidates belonging to BCS class-II. The racemic solids have been classified into three type based on melting point phase diagram. One of the most common types is racemic compound which having a definite number of molecules of each enantiomer in the unit cell of the crystal and poses one phase crystalline addition compound. Two eutectics of different compositions have been found for an addition compound. Emphasis is being given to use of a binary product rather than a single one. In addition to thermodynamic and pharmacokinetic differences between pure and binary solid dispersions supports to use the solid dispersions in solid doses form in place of pure drug candidate. Nicotinamide is a water soluble vitamin B_3, a component of the vitamin B complex group. It was first time clinically used in measuring pellagra preventive factors[5] (PPF) and in treatment of patients undergoing radiation therapy[6] for lung tumors caused by Mycobacterium Tuberculosis. Intake of nicotinamide for the treatment of HIV-positive patients was suggested 3g per day as tolerable dose[7]. In addition it has not been shown to produce the flushing, itching and burning sensations of the skin as is commonly seen when large doses of niacin are administrated orally. Nicam gel[8] is most effective when applied to the skin, which helps to reduce the inflammation and redness of inflammatory acne. It is a very important coenzyme that helps our body produce energy and aids in the metabolism of lipids, like cholesterol and carbohydrates in many reactions occur in our body. p-Nitroaniline is a chromogenic molecule that is used as a dyestuff intermediate in industrial applications.[1] In biochemical research, enzyme assays utilize modified aminoacyl or peptidyl p-nitroanilines as substrates. The enzyme catalyzes the release of

* *To whom correspondence be made:*
E-mail: imvishnukant@gmail.com, hshe2503@rediffmail.com

free p-nitroaniline, which is the basis of the colorimetric determination of the enzyme activity.[9,10] Physical and chemical properties of solid dispersions can be understood to a great extent in terms of crystallite size, mechanical strength and thermodynamic properties. The fundamental knowledge of drug-excipient interactions and a comprehensive study of the thermal properties, structure and solubility of binary system is the prerequisite for the development of useful drug products. The present binary system NA-pNA has been investigated for a detailed thermodynamic and interfacial properties such as solid-liquid equilibrium, excess and mixing thermodynamic function, activity and activity coefficient, thermal stability, interfacial energy (σ), surface roughness (α), driving force of solidification (ΔG_v) and critical radius.

EXPERIMENTAL DETAILS

Nicotinamide (Thomas Baker, Bombey) and p-Nitroaniline (Loba, India) were directly taken for investigation. The melting point (experimental value) of nicotinamide was found 128°C while for p-Nitroaniline was found 144°C respectively. The solid-liquid equilibrium data of NA-pNA system were determined by the thaw-melt method[11,12] Mixtures of different composition were made in glass test tubes by repeated heating and followed by chilling in ice. The melting and thaw temperatures were determined in a Toshniwal melting point apparatus using a precision thermometer which could read correctly up to ± 0.1°C. The heater was regulated to give above 1°C increase in temperature in every five minutes. Heat of fusion of materials was measured by the DTA method using NETZSCH Simultaneous Thermal Analyzer, STA 409 series unit. All the runs were carried out with heating rate 2°C/min, chart speed 10mm/min and chart sensitivity 100μv/10mv.The sample weight was 5 mg for all estimation. Using benzoic acid was a standard substance, the heat of fusion of unknown compound was determined[13,14] using the following equation:

$$\Delta H_x = \frac{\Delta H_s W_s A_x}{W_s A_x}$$

where ΔH_x is the heat of fusion of unknown sample and ΔH_s is the heat of fusion of standard substance. W and A are weight and peak area, respectively and suffices x and s indicate the corresponding quantities for the unknown and standard substances, respectively.

RESULTS AND DISCUSSION

Thermodynamic Study

Phase diagram

Solid-liquid equilibrium data of NA-pNA system determined by the thaw melt method, is reported (Table 1) and shown in the form of temperature-composition curve in Fig. 1. Solid-liquid phase diagram exhibits eutectic behaviour at 0.420 mole fraction of p-nitroaniline at 102°C melting temperature and a 1:4 additive co-crystal with incongruent melting at 131°C with a peritectic 0.674 mole fraction of p-nitroaniline at 130°C. The incongruent melting and a undefined inclination in the intermediate region at the top of the curve in the diagram suggest the instability but actual stoichiometry of the crystal formed. At the eutectic temperature two phases namely a liquid phase L and two solid phases (S_1 and S_2) are in equilibrium and the system is invariant. In the region indicated by L a homogenous binary liquid solution exists while the two solid phases exists below the horizontal line. In the case, in region located on the left side of the diagram a binary liquid and solid NA exist while in a similar region located on the right side of the diagram a binary liquid and the second component of the system co-exist, which is represented as :

$$L \underset{\text{Cooling}}{\rightleftharpoons} S_1 + S_2$$

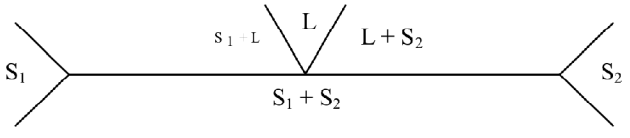

In peritectic S_1 + L on undercooling gives S_2 and represented as:

$$S_1 + L \underset{\text{Cooling}}{\rightleftharpoons} S_2$$

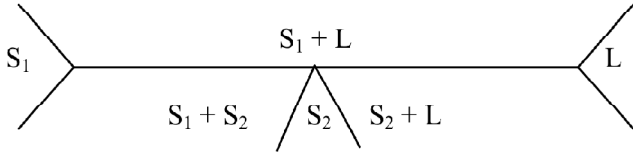

Table 1
Phase composition, melting temperature, values of enthalpy of fusion (DH), entropy of fusion (DS), roughness parameter (A), interfacial energy and Gibbs Thomson coefficient (t)

Solid Dispersions	χ_{NA}	*MP (°C)*	ΔH *(J/mol)*	ΔS *(J/mol/K)*	α	σ *(kJ/m²)*	σ_{gb} *(kJ/m²)*	ΔS_v *kJ/m³/K*	$t \times 10^6$ *Km*
NA		128	25400.00	63.34	7.62	50.46	97.48	726	6.95
pNA		144	21506.00	51.57	6.20	39.81	76.90	532	7.94
A1	0.112	140	21942.13	53.13	6.39	40.92	79.06	554	7.39
A2	0.200	131	22284.80	55.16	6.63	41.81	80.78	580	7.20
A3	0.326	130	22775.44	56.51	6.80	43.11	83.27	602	7.16
A4	0.430	126	23180.42	58.10	6.99	44.19	85.37	626	7.06
A5	0.531	115	23573.71	60.76	7.31	45.26	87.44	662	6.84
E	0.580	102	23764.52	63.37	7.62	45.79	88.46	694	6.60
A6	0.610	103	23881.34	63.51	7.64	46.11	89.08	698	6.61
A7	0.677	106	24142.24	63.70	7.66	46.84	90.49	705	6.65
A8	0.725	111	24329.15	63.36	7.62	47.37	91.50	705	6.72
A9	0.819	116	24695.19	63.48	7.64	48.41	93.52	713	6.79
A10	0.911	121	25053.43	63.59	7.65	49.44	95.52	722	6.85

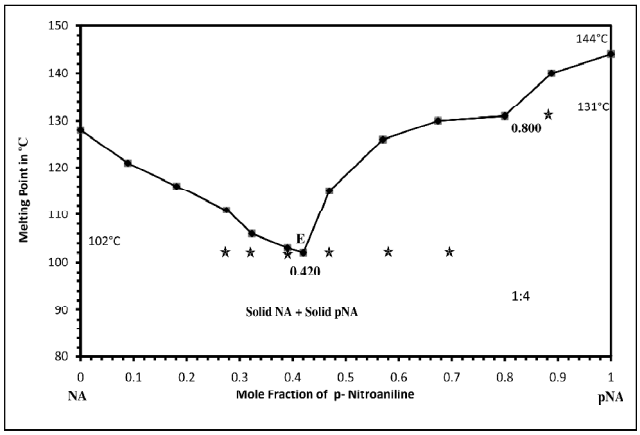

Figure 1: Phase Diagram of Nicotinamide - p-Nitroaniline system

Heat of Fusion

The values of heats of fusion of eutectic and non-eutectic solid dispersions are calculated by the mixture law using equation

$$(\Delta H)_e = \chi_{NA}\ \Delta H_{NA} + \chi_{pNA}\ \Delta H_{pNA} \qquad (1)$$

where χ and ΔH are the mole fraction and the heat of fusion of the component indicated by the subscript, respectively. The value of heat of fusion of binary products A1-A10 and E is reported in Table 1.

Mixing Functions

Integral molar free energy of mixing (ΔG^M), molar entropy of mixing (ΔS^M) and molar enthalpy of mixing (ΔH^M) and partial thermodynamic mixing functions of the binary alloys when two components are mixed together were determined by using the following equations

$$\Delta G^M = RT\ (\chi_{NA}\ lna^l_{NA} + \chi_{pNA}\ lnal_{pNA}) \qquad (2)$$

$$\Delta S^M = -R\ (\chi_{NA}\ lnx^l_{NA} + \chi_{pNA}\ ln\chi l_{pNA}) \qquad (3)$$

$$\Delta H^M = RT\ (\chi_{NA}\ lng^l_{NA} + \chi_{pNA}\ lng^l_{pNA}) \qquad (4)$$

$$G_i^{-M} = \mu_i^{-M} = RT\ lna^l_i \qquad (5)$$

where G_i^{-M} (μ_i^{-M}) is the partial molar free energy of mixing of component i (mixing chemical potential) in binary mix. and γ_i and a_i is the activity coefficient and activity of component respectively. The negative value[15,16] of integral molar free energy of mixing of all the eutectic and non-eutectic solid dispersions (Table 2) suggests that the mixing in all cases is spontaneous. The integral molar enthalpy of mixing value corresponds to the value of excess integral molar free energy of the system favors the regularity in the binary solutions.

The activity coefficient/activity of components for the systems has been calculated from the equation[13] given below

$$-\ln\chi_i^1\gamma_i^1 = \frac{\Delta H_i}{R}\left(\frac{1}{T_e} - \frac{1}{T_i}\right) \qquad (6)$$

where γ_i^1 is activity coefficient of the component i in the liquid phase respectively, ΔH_i is the heat of fusion of component i at melting point T_i and R is

Table 2
Value of partial and integral mixing of Gibbs free energy (ΔG^M), enthalpy (ΔH^M) and entropy (ΔS^M) of NA-pNA system

Solid Dispersions	ΔG_{NA}^{-M} J/mol	ΔG_i^{-M} J/mol	ΔG^M J/mol	ΔH_{NA}^{-M} J/mol	ΔH_i^{-M} J/mol	ΔH^M J/mol	ΔS_{NA}^{-M} J/mol/K	ΔS_i^{-M} J/mol/K	ΔS^M J/mol/K
A1	760.10	-206.29	-98.06	8277.31	3641.29	-1106.05	10.50	0.99	2.92
A2	190.02	-670.45	-498.36	5595.90	3438.85	-1182.42	9.92	1.86	4.16
A3	126.68	-722.02	-445.35	3882.16	4007.44	-1669.88	9.43	3.28	5.25
A4	-126.68	-928.32	-583.61	2673.01	4399.20	-1683.14	9.16	4.67	5.68
A5	-823.44	-1495.62	-1138.69	1218.49	4326.26	-1091.08	8.95	6.29	5.75
E	-1646.88	-2166.07	-1864.94	51.44	3705.64	-256.04	8.86	7.21	5.66
A6	-1583.54	-2114.50	-1790.61	-38.34	4075.42	-299.93	8.81	7.83	5.56
A7	-1393.52	-1959.78	-1576.42	-164.36	5237.64	-405.91	8.70	9.40	5.23
A8	-1076.81	-1701.91	-1248.71	-50.13	6812.28	-629.06	8.64	10.73	4.89
A9	-760.10	-1444.05	-883.89	-114.33	11433.21	-645.55	8.51	14.21	3.93
A10	-443.39	-1186.18	-509.50	-138.05	25624.31	-473.93	8.41	20.11	2.50

the gas constant. T_e is the melting temperature of solid dispersions. Using the values of activity and activity coefficient of the components in alloys mixing and excess thermodynamics functions have been computed.

Excess thermodynamic functions

With a view to have a quantitative idea and nature of molecular interactions between the components forming the eutectic and non-eutectic solid dispersions, the excess thermodynamic functions such as excess integral free energy (g^E), excess integral entropy (s^E) and excess integral enthalpy (h^E) were calculated using the following equations

$$g^E = RT(\chi_{NA} \ln \gamma^l_{NA} + \chi_{pNA} \ln \gamma^1_{pNA}) \quad (7)$$

$$s^E = -R\left((\chi_{NA} \ln \gamma^1_{NA} + \chi_{pNA} \ln \gamma^1_{pNA} + \chi_{NA} T \frac{\delta \ln \gamma^1_{NA}}{\delta T} + \chi_{pNA} T \frac{\delta \ln \gamma^1_{pNA}}{\delta T} \right) \quad (8)$$

$$h^E = -RT^2 \left(\chi_{NA} \frac{\delta \ln \gamma^1_{NA}}{\delta T} + \chi_{pNA} \frac{\delta \ln \gamma^1_{pNA}}{\delta T} \right) \quad (9)$$

and excess chemical potential or excess partial free Gibbs energy

$$g_i^{-E} = \mu_i^{-E} = RT \ln \gamma^1_i \quad (10)$$

The values of $\delta \ln \gamma_i^1 / \delta T$ can be determined by the slope of liquidus curve near the alloys form in the phase diagram. The values of the excess thermodynamic functions are given in Table 3. The value of the excess integral free energy is a

Table 3
Value of partial and integral excess Gibbs free energy (g^E), enthalpy (h^E) and entropy (s^E) of NA-pNA system

Solid Dispersions	$g_{NA}^{-EJ/mol}$	$g_{pNA}^{-EJ/mol}$	$g^{EJ/mol}$	$h_{NA}^{-EJ/mol}$	$h_{pNA}^{-EJ/mol}$	$h^{EJ/mol}$	$s_{NA}^{-EJ/mol/K}$	$s_{pNA}^{-EJ/mol/K}$	$s^{EJ/mol/K}$
A1	8277.31	201.57	1106.05	189848.94	5642.52	26273.63	439.64	13.17	60.94
A2	5595.90	79.06	1288.66	89943.12	7329.78	23852.45	208.78	17.95	56.11
A3	3882.16	599.85	1669.88	140277.11	58628.62	85246.03	338.45	143.99	207.38
A4	2673.01	936.39	1683.14	26928.26	17969.70	21821.88	60.79	42.69	50.47
A5	1218.49	946.83	1091.08	-8900.26	-2825.06	-6050.99	-26.08	-9.72	-18.41
E	51.44	538.58	256.04	-10281.60	-628.21	-6227.18	-27.55	-3.11	-17.29
A6	-38.34	829.03	299.93	32406.56	68909.39	46642.66	86.29	181.06	123.25
A7	-164.36	1601.18	405.91	4588.08	41348.28	16461.63	12.54	104.87	42.36
A8	-50.13	2419.65	629.06	-8490.36	23073.97	189.83	-21.98	53.79	-1.14
A9	-114.33	4083.94	645.55	5322.41	117508.67	25628.13	13.98	291.58	64.22
A10	-138.05	6738.16	473.93	-4149.20	196016.26	13665.53	-10.18	480.40	33.48

measure of the departure of the system from ideal behavior. The reported excess thermodynamic data substantiate the earlier conclusion of an appreciable interaction during the formation of solid dispersions. The positive value[17,18] of excess free energy of all solid dispersions indicates the weaker association between unlike molecules. The excess entropy is a measure of the change in configurational energy due to a change in potential energy and indicates an increase in randomness.

Gibbs-Duhem equation

The partial molar free energy of mixing, activity and activity coefficient can also be determined by using Gibbs-Duhem equation[19]

$$\sum \chi_i dz_i^{-M} = 0 \qquad (11)$$

$$or \quad \chi_{NA} dH_{NA}^{-M} + \chi_{pNA} dH_{pNA}^{-M} = 0 \qquad (12)$$

$$or \quad dH_{NA}^{-M} = \frac{\chi_{pNA}}{\chi_{NA}} dH_{pNA}^{-M} \qquad (13)$$

$$or \quad [\mathrm{H}_{\mathrm{NA}}^{-\mathrm{M}}]_{\chi_{NA}=y} = \int_{\chi_{NA}=y}^{\chi_{NA}=1} \frac{\chi_{pNA}}{\chi_{NA}} dH_{pNA}^{-M} \qquad (14)$$

Using equation (14) a graph (Fig. 2) between H_{pNA}^{-M} and χ_{pNA}/χ_{NA} gives the solution of the partial molar heat of mixing of a constituent *NA* in *NA*/*pNA* solid dispersions and plot between $\ln\gamma_{pNA}$ vs χ_{pNA}/χ_{NA} determines the value of activity coefficient (Fig. 3) of component *NA* in binary solid dispersions.

Stability Function

Thermodynamic strength of the present system in form of stability and excess stability functions[20,21] can be determined by the second derivative of their molar free energy and excess energy respectively, with respect to the mole fraction of either constituent:

$$Stability = \frac{\partial^2 \Delta G^M}{\partial \chi^2} = -2RT \frac{\partial \ln a}{\partial (1-\chi)^2} \qquad (15)$$

$$Excess\ \ Stability = \frac{\partial^2 g^E}{\partial \chi^2} = -2RT \frac{\partial \ln \gamma}{\partial (1-\chi)^2} \qquad (16)$$

These values may be calculated by multiplying the slope of ln*a* vs $(1-\chi)^2$ and lng vs $(1-\chi)^2$ plots

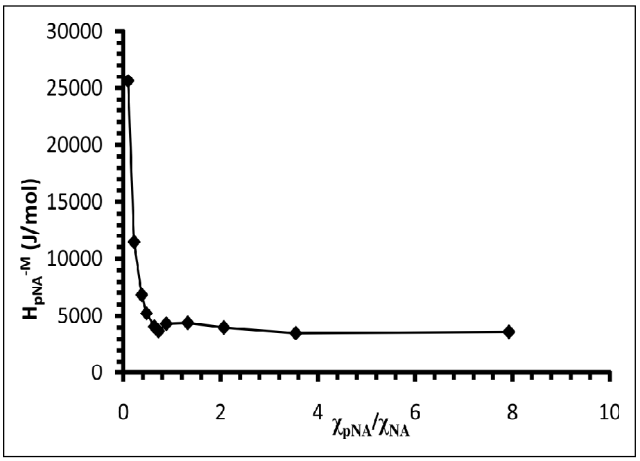

Figure 2: Graphical solution of partial molar enthalpy of mixing of pNA in binary mix

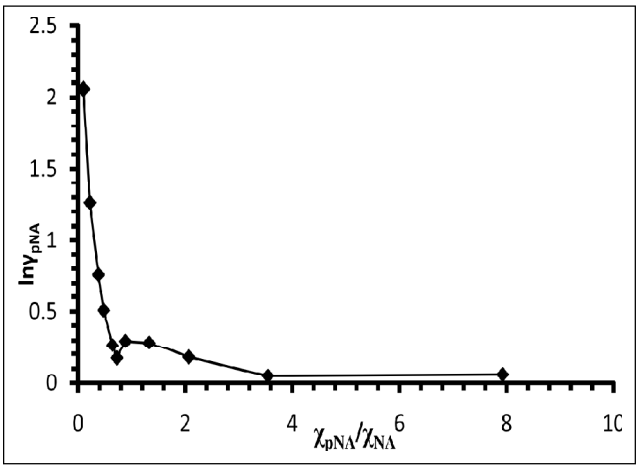

Figure 3: Graphical solution of activity coefficient of pNA in binary mix

with -2RT. The best polynomial equation of the curve generated is given below:

$$\ln\gamma = 3.68(1-\chi)^2 - 21.44(1-\chi)^4 + 81.99(1-\chi)^6 - 146.84(1-\chi)^8 + 126.(1-\chi)^{10} - 41.47(1-\chi)^{12} \qquad (17)$$

The slope of the curve shown in Fig. 4 as obtained by differentiating the above equation with respect to $(1-x)^2$ may also be used to calculate the excess stability of the NA-pNA system. The values of total stability to the ideal stability and defined as

$$Ideal\ Stability = \frac{RT}{\chi(1-\chi)} \qquad (18)$$

These values show the overall thermodynamic stability in the solid dispersions.

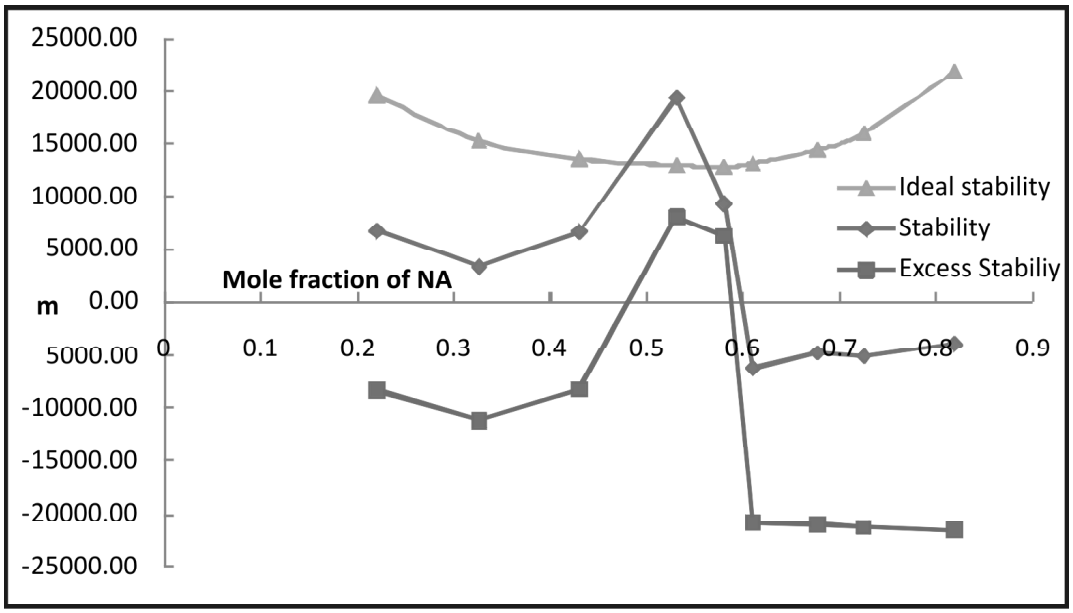

Figure 4: Stability Function of NA-pNA System

Interfacial Studies

The effective entropy change (ΔS_v)

The effective entropy change and the volume fraction of phases in the alloy have key role in controlling and deciding the interface morphology during solidification and the volume fraction of the two phases depends on the ratio of effective entropy change of the phases. The entropy of fusion ($\Delta S = \Delta H / T$) value (Table 1) of alloys is calculated by heat of fusion values of the materials. The effective entropy change per unit volume (ΔS_V) is given by

$$\Delta S_V = \frac{\Delta H}{T} \cdot \frac{1}{V_m} \tag{19}$$

where ΔH is the enthalpy change, T is the melting temperature and V_m is the molar volume of solid phase. The entropy of fusion per unit volume (ΔS_V) for NA and pNA was found 726 and 532 $kJK^{-1}m^{-3}$ respectively. Values of ΔS_V for alloys are reported in Table 1.

The solid-liquid interfacial energy (s)

An important thermo-physical property is responsible for growth interface. It has been very difficult to measure it with accuracy through experiments and an experimentally observed value of interfacial energy 'σ' keeps a variation of 50-100% from one worker to other. However, Singh and Glickman[22] had calculated the solid-liquid interfacial energy (σ) from the value of melting enthalpy change and values obtained were found in good agreement with the experimental values. Turnbull empirical relationship[23] between the interfacial energy and enthalpy change provides the clue to determine the interfacial energy value of alloy and is expressed as:

$$\sigma = \frac{C\Delta H}{(N)^{1/3}(V_m)^{2/3}} \tag{20}$$

where the coefficient C lies between 0.33 to 0.35 for nonmetallic system, V_m is molar volume and N is the Avogadro's constant. The value of the solid-liquid interfacial energy of nicotinamide and p-nitroaniline was found to be 50.46 and 39.81 kJm^{-2} respectively and σ value of solid dispersions was given in Table 1.

Interfacial energy can also be calculated by using Gibbs-Thomson coefficient (τ). For a planar grain boundary on planar solid-liquid interface the τ value coefficient for the system can be calculated by the Gibbs-Thomson equation is expressed as

$$\tau = r\Delta T = \frac{TV_m\sigma}{\Delta H} = \frac{\sigma}{\Delta S_V} \tag{21}$$

where τ is the Gibbs-Thomson coefficient, ΔT is the dispersion in equilibrium temperature and, r is the radius of grooves of interface. The theoretical basis of determination of τ was made for equal thermal conductivities of solid and liquid phases

for some transparent materials. It was also determined by the help of Gunduz and Hunt numerical method[24] for materials having known grain boundary shape, temperature gradient in solid and the ratio of thermal conductivity of the equilibrated liquid phases to solid phase ($R = K_L/K_S$). The Gibbs-Thomson coefficient for NA, p-NA and their solid dispersions are found in the range of 6.60-7.94 x 10^{-06} Km and is reported in Table 1.

The driving force of nucleation (DG_v)

The various solidification processes have been focused in the light of diffusion model, kinetic theory of nucleation and thermodynamic laws. Previously it has been explained that the lateral motion of rudementry steps in liquid advances stepwise/ nonuniform surface at low driving force while continuous and uniform surface advances at sufficiently high driving force. The driving force of nucleation during solidification (ΔG_V) is determined at under cooling (ΔT) by using the following equation[25]

$$\Delta G_V = \Delta S_v \Delta T \qquad (22)$$

It is opposed by the increase in surface free energy due to creation of a new solid-liquid interface. By assuming that solid phase nucleates as small spherical cluster of radius arising due to random motion of atoms within liquid. The value of ΔG_V is shown in the Table 4.

The critical size of nucleus (r)*

It is well known that during liquid-solid transformation embryos (unstable nucleus) are rapidly dispersed in unsaturated liquid and on undercooling liquid becomes saturated and provides particles with stable nucleus corresponding to size of critical nucleus which is responsible for the nucleation and growth of crystal. The radius of critical nucleus /critical size of nucleus (r*) can be expressed by the Chadwick relation[26]

$$r^* = \frac{2\sigma}{\Delta G_V} = \frac{2\sigma T}{\Delta H_V \Delta T} \qquad (23)$$

where σ is the interfacial energy and ΔH_V is the enthalpy of fusion of the compound per unit volume, respectively. The critical size of the nucleus for the components and alloys was calculated at different undercoolings and values are presented in Table 5. It can be inferred from table that the size of the critical nucleus decreases with increase in the undercooling of the melt. The existence of embryo and a range of embryo size can be expected in the liquid at any temperature.

Further it has been observed that during critical nucleus formation, a localized critical free energy of nucleation (ΔG^*) is required which is evaluated[27] as

Table 4
Value of volume free energy change (ΔG_v) during solidification for NA - pNA system at different undercoolings (ΔT)

Solid Dispersions $\Delta T \longrightarrow$	ΔG_v *(kJ/m³)*					
	1.0	*1.5*	*2.0*	*2.5*	*3.0*	*3.5*
NA	0.726	1.089	1.452	1.815	2.178	2.541
pNA	0.532	0.798	1.063	1.329	1.595	1.861
A1	0.554	0.831	1.108	1.385	1.662	1.939
A2	0.580	0.871	1.161	1.451	1.741	2.031
A3	0.602	0.904	1.205	1.506	1.807	2.108
A4	0.626	0.939	1.252	1.565	1.878	2.191
A5	0.662	0.993	1.324	1.654	1.985	2.316
E	0.694	1.041	1.388	1.735	2.082	2.428
A6	0.698	1.046	1.395	1.744	2.093	2.442
A7	0.705	1.057	1.409	1.762	2.114	2.467
A8	0.705	1.057	1.409	1.761	2.114	2.466
A9	0.713	1.070	1.427	1.783	2.140	2.496
A10	0.722	1.083	1.443	1.804	2.165	2.526

Table 5
Critical size of nucleus (r*) at different undercoolings (ΔT)

Solid Dispersions	*r*(nm)*					
ΔT ⟶	*1.0*	*1.5*	*2.0*	*2.5*	*3.0*	*3.5*
NA	138.99	92.66	69.49	55.60	46.33	39.71
pNA	149.74	99.82	74.87	59.89	49.91	42.78
A1	147.74	98.49	73.87	59.10	49.25	42.21
A2	144.09	96.06	72.04	57.64	48.03	41.17
A3	143.11	95.41	71.55	57.24	47.70	40.89
A4	141.18	94.12	70.59	56.47	47.06	40.34
A5	136.80	91.20	68.40	54.72	45.60	39.08
E	131.98	87.99	65.99	52.79	43.99	37.71
A6	132.19	88.13	66.10	52.88	44.06	37.77
A7	132.93	88.62	66.46	53.17	44.31	37.98
A8	134.45	89.63	67.22	53.78	44.82	38.41
A9	135.73	90.49	67.87	54.29	45.24	38.78
A10	137.02	91.34	68.51	54.81	45.67	39.15

$$\Delta G^* = \frac{16}{3}\frac{\pi\sigma^3}{\Delta G_v^2} \qquad (24)$$

The value of ΔG* has been found in the range of 10^{-15} to 10^{-16} J per molecule at undercoolings 1-3.5°K, and has been reported in Table 6.

Interfacial Grain boundary energy (σ_{gb})

During in liquid-solid transformation nucleation and growth on internal surfaces gives the idea about fundamentals of grain boundary. In past, a numerical method[28] is applied to observe the interfacial grain boundary energy (σ_{gb}) without applying the temperature gradient for the grain boundary groove shape. For isotropic interface there is no difference in the value of interfacial tension and interfacial energy. A considerable force is employed at the grain boundary groove in anisotropic interface. The grain boundary energy can be obtained by the equation:

$$\sigma_{gb} = 2\sigma \cos\theta \qquad (25)$$

where θ is equilibrium contact angle precipitates at solid-liquid interface of grain boundary. The grain boundary energy could be twice the solid-

Table 6
Value of critical free energy of nucleation (ΔG*) for alloys of NA-pNA system at different undercooling (ΔT)

Solid Dispersions *ΔT* ⟶	*ΔG*´10¹⁶ (J/molecule)*					
	1.0	*1.5*	*2.0*	*2.5*	*3.0*	*3.5*
NA	40.85	18.15	10.21	6.54	4.54	3.33
pNA	37.40	16.62	9.35	5.98	4.16	3.05
A1	37.43	16.64	9.36	5.99	4.16	3.06
A2	36.38	16.17	9.09	5.82	4.04	2.97
A3	36.99	16.44	9.25	5.92	4.11	3.02
A4	36.91	16.40	9.23	5.91	4.10	3.01
A5	35.49	15.77	8.87	5.68	3.94	2.90
E	33.42	14.85	8.36	5.35	3.71	2.73
A6	33.77	15.01	8.44	5.40	3.75	2.76
A7	34.68	15.41	8.67	5.55	3.85	2.83
A8	35.88	15.95	8.97	5.74	3.99	2.93
A9	37.37	16.61	9.34	5.98	4.15	3.05
A10	38.90	17.29	9.72	6.22	4.32	3.18

liquid interfacial energy in the case where the contact angle tends to zero. The value of σ_{gb} for solid NA and pNA was found to be 97.48 and 76.90 kJm^{-2} respectively and the value for all solid dispersions is given in Table 1.

Interface Morphology

The solid-liquid interface morphology can be predicted from the value of the entropy of fusion. According to Hunt and Jackson[29], the type of growth from a binary melt depends upon a factor á which is almost the entropy of fusion in dimensionless unit, defined precisely:

$$\alpha = \xi \frac{\Delta H}{RT} = \xi \frac{\Delta S}{R} \qquad (26)$$

where $\xi\{T_c / T = (T - DT) / T\}$ is a crystallographic factor depending upon the geometry of the molecules and has a value less than or equal to one. $\Delta S / R$ (also known as Jackson's roughness parameter α) is the entropy of fusion (dimensionless) and R is the gas constant. When á is less than 2 for both phases the solid-liquid interface essentially grow from the melt isotropically with no crystalline facets transforming the melt into regular crystalline morphology and becomes atomically rough and exhibits non-faceted growth. Irregular interface appears when $\alpha > 2$ for both phases, which concurrently initiate the anisotropic growth with crystalline facets. The non-faceted crystal holds a round growth front while the faceted crystal poses a sharp growth front. The computed a values for nicotinamide and p-nitroaniline respectively are on the order of 7.62 and 6.20 revealing the faceted morphology of the binary composite material. The microstructures of pure NA and pNA have been shown in Fig. 5 & 6. The microstructure of eutectic of NA-pNA system containing 0.42 mole fraction of pNA shows conglomerate morphology (Fig. 7). It is formed as a result of separate growth of eutectic phases. In this morphology there is co-existance of eutectic phases in a particular region. This may be due to difference of undercooling and growth rate of the phase and leading one of phases followed by other phase in the eutectic. Additive co-crystal (1:4) of NA-pNA system (Fig. 8) exhibits complex regular having lamellar morphology. It is observed as a result of an energy barrier that exists for the addition of new solid layer during solidification which proceeds by the lateral movement of steps across a specific

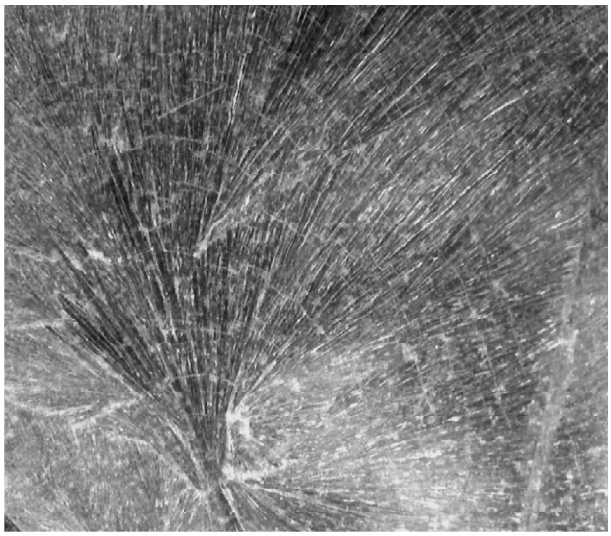

Figure 5: Microstructure of Pure Nicotinamide (NA) x 50

Figure 6: Microstructure of Pure p-Nitroaniline (pNA) x 50

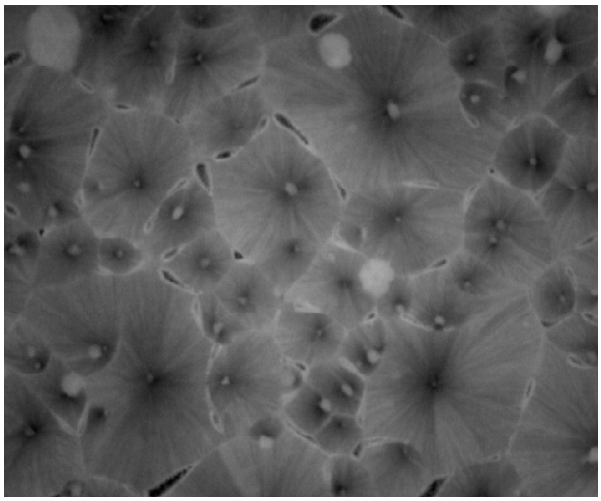

Figure 7: Microstructure of Eutectic of NA-pNA system x 230

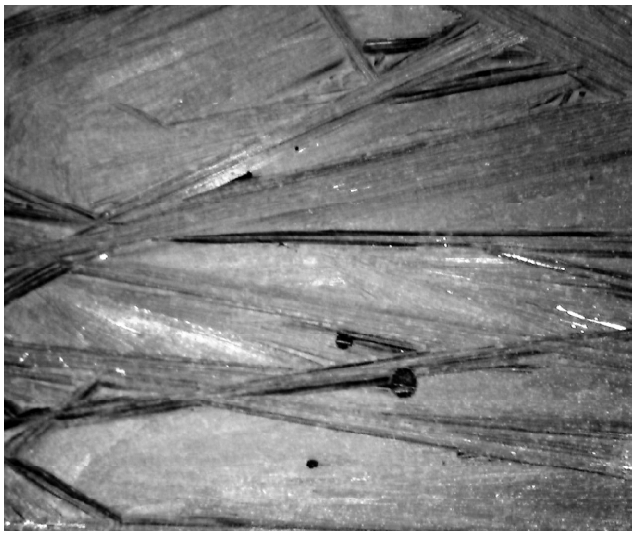

Figure 8: Microstructure of Addition (1:4) of NA-pNA system x 50

crystallographic facet plane. The liquid-solid growth habits of the overall binary products due to their high entropies of fusion are greatly influenced by thermal and mechanical stresses and splitted into groups of crystals that gives rise to a regular morphology. The value of Jackson's roughness parameter (α) is given in Table 1. For all the solid dispersions the a value was found greater than 2 which indicate the faceted[27] growth proceeds in all the cases.

Acknowledgement

Thanks are due to the Head Department of Chemistry, V K S University Ara 802301, India for providing research facilities.

References

[1] L. M. Oberoi, K. S. Alexander and A. T. Riga, Study of interaction between ibupro-fen and nicotinamide using differential scanning calorimetry, spectroscopy, and microscopy and formulation of a fast-acting and possibly better ibuprofen suspension for osteoarthritis patients, *J. Pharm. Sci.*, 94, **2005**, 93–101.

[2] R. E. Coffman and D. O. Kildsig, Effect of nicotinamide and urea on the solubility of riboflavin in various solvents, *Journal of Pharmaceutical Sciences*, 85(9), **1996**, 951–954.

[3] S.E. Bartsch and U. J. Griesser, Phycochemical Properties of the Binary System Glibenclamide and Polyethylene Glycol 4000, *J. Therm. Anal. Cal.*, 77, **2004**, 555-569.

[4] Shekhar H. and Kant Vishnu, Thermodynamics of Nicotinamide Based Binary Drug Systems, Lambert Academic Publishing, Germany, **2013**.

[5] Uber, den Tanner **(1951)**. Versuch einer neuer medikamentosen Therapie der Bronchustuberkulose. *Helv Med Acta., 18*, 456–60.

[6] Jordahl, C., Desprez, R., Muchenheim, C., Deuschle, K. & McDermott, W., **(1961)**. Ineffectiveness of nicotinamide and isoniazid in treatment of pulmonary tuberculosis. *Am Rev Respir Dis. 83*, 899–901.

[7] Murray, M. F., Langan, M. & MacGregor, R. R., **(2001)**. Increased plasma tryptophan in HIV-infected patients treated with pharmacologic doses of nicotinamide. *Nutrition. 17,* 654–656.

[8] Hakozaki T, Minwalla L and Zhung J. **(2002)**. The effect of nicotinamide on reducing cutaneous pigmentation and suppression of melanosome transfer. *Br. J. Dermatol. 147*, 20-31.

[9] Wang, Q. M., *et al.*, A continuous colorimetric assay for rhinovirus-14 3C protease using peptide p-nitroanilides as substrates. Anal. Biochem., 252(2), 238-245 **(1997)**.

[10] Hou, W. C., *et al.*, Detection of protease activities using specific aminoacyl or peptidyl p-nitroanilides after sodium dodecyl sulfate - polyacrylamide gel electrophoresis and its applications. Electrophoresis, 20(3), 486-490 **(1999)**.

[11] J. Sangster, Phase diagram and thermodynamic properties of binary systems of drugs, *J. Phy. Chem. Data,* 28, 889-931, **(1999)**.

[12] Shekhar, H., Pandey, K. B. & Kant, Vishnu. **(2010)**. Thermodynamic Characteristics of 1:2 molecular complex of Phthalic anhydride-Camphene system. *J. Nat. Acd. Sci. Letter. 33*, 153-160.

[13] J. Charles Williamson, Interactive Two-Component Phase Diagrams, *J. Chem. Educ.*, 86(5), **2009**, 653.

[14] Krajewska-Cizio, A. **(1990)**. Phase Diagrams in the Binary Systems of N-isopropylcarbazole with 2,4,7-trinitrofluorene-9 on and carbazole. *Thermochimica Acta.158*, 317-25.

[15] H. Shekhar, Jaisheel Kumar1 and C. S. Saha2, Thermodynamic and Interfacial Studies of Co-crystals of 8- Hydroxyquioniline – Urea System, *Malaysian Journal of Chemistry*, **2013**, 15(1), 067 – 076.

[16] Nieto, R., Gonozalez, M. C. & Herrero, F. **(1999)**. Thermodynamics of mixtures, Function of mixing and excess functions, *American Journal of Physics. 67,* 1096-1099.

[17] Sharma, B. L., Tandon, S. & Gupta, S. **(2009)**. Characteristics of the binary faceted eutectic; benzoic Acid-Salicylic Acid system. *Cryst Res Technol. 44,* 258-268.

[18] H. Shekhar and Vishnu Kant, Thermodynamic Studies on Solid Dispersions, of Nicotinamide – Khellin Drug System, Mol. Cryst. Liq. Cryst., 577, 103–115, **2013**.

[19] Shamsuddin, M., Singh, S. B. & Nasar, A. **(1998)**. Thermodynamic investigations of liquid gallium-cadmium alloys. *Thermochemica Acta. 316*, 11-19.

[20] Darken, L. S. **(1967)**. Thermodynamics binary metallic solutions. *Trans Met Soc AIME. 239,* 80-89.

[21] Gupta, P., Agrawal, T., Das, S. S. & Singh, N. B. **(2012)**. Phase equilibria and molecular interaction studies on (naphthols + vanillin) systems, *J. Chem Thermody. 48*, 291-299.

[22] Singh, N. B. & Glicksman, M. E. **(1989)**. Determination of the mean solid-liquid interface energy of pivalic acid. *J Cryst Growth. 98,* 573-580.

[23] Turnbull, D. **(1950)**. Formation of Crystal Nuclei in Liquid Metals. *J. Chem. Phys. 21*, 1022-1027.

[24] Gunduz, M. & Hunt, J. D. **(1989)**. Solid-Liquid surface energy in the Al-Mg system. *Acta Metall. 37,* 1839-1845.

[25] Shekhar, H. & Kant, Vishnu. **(2013)**. Thermal and Interfacial Studies of Binary Alloys of Nicotinamide - b-Naphthol Drug System. *Asian Journal of Chemistry. 25 (5),* 2441-2446.

[26] Chadwick, G. A. **(1972)**. Metallography of Phase Transformation. Butterworths; London: p.61.

[27] Wilcox, W. R. **(1974)**. The relation between classical nucleation theory and the solubility of small particles. *Journal of crystal growth. 26,* 153-154.

[28] Akbulut, S., Ocak, Y., Keslioglu, K. & Marasli, N. **(2009)**. Determination of Interfacial Energies in the Aminomethylpropanediol-neopentylglycol Organic Alloy. *Applied Surface Science. 255,* 3594-99.

[29] Hunt, J. D. & Jackson, K. A. **(1966)**. Binary Eutectic Solidification. *Trans Metall Soc AIME. 236,* 843-852.